Dynamic Structure Factor of Polystyrene and Poly(methyl methacrylate) in Θ Solvents

Nobuo Sawatari, Takenao Yoshizaki, and Hiromi Yamakawa*

Department of Polymer Chemistry, Kyoto University, Kyoto 606-8501, Japan

Received March 6, 1998; Revised Manuscript Received April 21, 1998

ABSTRACT: The dynamic structure factor and its first cumulant $\Omega(k)$ as functions of the magnitude k of the scattering vector were determined from dynamic light scattering (DLS) measurements for two atactic polystyrene samples having the weight-average molecular weights $M_w = 6.40 \times 10^6$ and 8.04×10^6 in cyclohexane at 34.5 °C (Θ) and for two atactic poly(methyl methacrylate) samples having $M_w = 4.82 \times 10^6$ and 1.31×10^7 in acetonitrile at 44.0 °C (Θ). The translational diffusion coefficient and the mean-square radius of gyration $\langle S^2 \rangle$ were also determined from DLS and static light scattering measurements, respectively, for all the samples except for the a-PS sample with the smaller M_w. It is found that even in such a range of large M_w, the "universal" behavior cannot be realized; i.e., the plot of $\eta_0\Omega(k)/k_BTk^3$ against $\langle S^2 \rangle^{1/2}k$ depends on the kind of polymer in the k^3 -region, where η_0 is the solvent viscosity, k_B the Boltzmann constant, and T the absolute temperature. This result is consistent with the theoretical prediction on the basis of the helical wormlike (HW) chain model, although the HW theory cannot quantitatively explain the experimental data for the individual polymer.

Introduction

There have already been performed many experimental investigations on the first cumulant Ω of the dynamic structure factor of flexible chain polymers with very high molecular weights in Θ solvents. Most of them were aimed to confirm the universal behavior of Ω as a function of the magnitude k of the scattering vector. Here, by the term "universal" we mean that the plot of $\eta_0\Omega(k)/k_BTk^3$ against $\langle S^2 \rangle^{1/2}k$, especially its height in an intermediate range of k, is independent of the polymer−solvent system, where η_0 is the solvent viscosity, k_B the Boltzmann constant, T the absolute temperature, and $\langle S^2 \rangle$ the mean-square radius of gyration. This is just the prediction by the Gaussian chain theory.[1−3] Very recently, however, it has been shown on the basis of the helical wormlike (HW) chain model[4] that the above plot may depend on the kind of polymer even for large molecular weights.[5] The purpose of the present paper is to examine experimentally whether this is the case or not.

For this purpose, it is suitable to make a comparison between experimental data for Ω for atactic polystyrene (a-PS) and atactic poly(methyl methacrylate) (a-PMMA), since these two polymer chains are remarkably different from each other in chain stiffness and local chain conformation.[4] We note that the above prediction for the HW chain is due to the numerical results for these two polymers.[5] Although a number of dynamic light scattering (DLS) measurements of Ω have already been reported for a-PS in Θ solvents, we carry out similar measurements for this polymer in cyclohexane at 34.5 °C (Θ) as well as for a-PMMA in acetonitrile at 44.0 °C (Θ). The reasons for this are that it is known that an experimental determination of $\Omega(k)$ in the intermediate range of k is rather sensitive to choice of the sampling time[6,7] and that it also seems to depend, to some extent, on the data processing procedure adopted for its evaluation from photon-correlation data. For the present purpose, therefore, it is desirable to compare experimental values of $\Omega(k)$ determined following the same procedure in the same laboratory.

As mentioned above, there remain some experimental ambiguities in the determination of $\Omega(k)$, i.e., the initial decay rate of the photon-correlation function, from experimental values of the function directly observed. Thus, in order to draw a definite conclusion free of such possible errors, we also make a direct comparison between the reduced photon-correlation functions for the two polymers.

Experimental Section

Materials. The two a-PS samples used in this work are those obtained from the original standard ones F-550 and F-850 supplied by Tosoh Co., Ltd. The sample from F-550, which is designated F550-a, is the same as that used in the previous study of the hydrodynamic-radius expansion factor,[8] and the sample designated F850-a is a fraction separated from F-850 by fractional precipitation. They have a fixed stereochemical composition (the fraction of racemic diads $f_r = 0.59$). The two a-PMMA samples used are the fractions separated by fractional precipitation from the original samples prepared by radical polymerization in bulk at 60 °C, both having $f_r = 0.79$.

The solvents cyclohexane and toluene for a-PS and acetonitrile and acetone for a-PMMA were purified according to standard procedures prior to use.

Static Light Scattering. Static light scattering (SLS) measurements were carried out to determine the weight-average molecular weight M_w and $\langle S^2 \rangle$ for the a-PS sample F850-a in cyclohexane at 34.5 °C (Θ) and for the two a-PMMA samples in acetonitrile at 44.0 °C (Θ). Measurements were also carried out to determine M_w for the two a-PS samples in toluene at 15.0 °C and for the two a-PMMA samples in acetone at 25.0 °C. A Fica 50 light-scattering photometer was used for all the measurements with vertically polarized incident light of wavelength 436 nm. For a calibration of the apparatus, the intensity of light scattered from pure benzene was measured at 25.0 °C at a scattering angle of 90°, where the Rayleigh ratio $R_{Uu}(90°)$ of pure benzene was taken as 46.5×10^{-6} cm^{-1}. The depolarization ratio ρ_u of pure benzene at 25.0 °C was found to be 0.41±0.01. Scattering intensities were measured at five different concentrations and at scattering angles ranging from 15 to 85°. All the data obtained were analyzed by the Berry square-root plot.[9]

The most concentrated solutions of the samples were allowed to stand in the dark at ca. 50 °C for 10 days for F850-a

S0024-9297(98)00354-4 CCC: $15.00
Published on Web 05/29/1998

Table 1. Values of M_w, M_w/M_n, $\langle S^2\rangle^{1/2}$, and R_H for Polystyrene and Poly(methyl methacrylate)

sample	M_w	M_w/M_n	$10^{-2}\langle S^2\rangle^{1/2}$, Å	$10^{-2} R_H$, Å
a-PS ($f_r = 0.59$) in Cyclohexane at 34.5 °C (Θ)				
F550-a[a]	6.40×10^6 (6.36×10^6)[b]		7.2_8	5.5_3
F850-a	8.04×10^6 (8.13×10^6)		8.2_2	6.3_0
a-PMMA ($f_r = 0.79$) in Acetonitrile at 44.0 °C (Θ)				
Mr48	4.86×10^6 (4.79×10^6)	1.09	5.7_0	4.4_3
Mr127	1.31×10^7 (1.27×10^7)		9.3_9	7.2_5

[a] The values of M_w, $\langle S^2\rangle^{1/2}$, and R_H for F550-a in cyclohexane at 34.5 °C have been reproduced from ref 8. [b] The values in parentheses represent the values of M_w determined from SLS measurements for a-PS in toluene at 15.0 °C and for a-PMMA in acetone at 25.0 °C.

in cyclohexane, at ca. 50 °C for 2 days for F850-a in toluene, and at ca. 50 °C for 2 days for a-PMMA in acetone, being stirred by shaking the vessel gently twice a day. Then optical purification was made by filtration through a Teflon membrane of pore size 1.0 μm for these solutions except for the a-PMMA sample Mr48 in acetone for which a membrane of pore size 0.45 μm was used. From a comparison between the flow times of the solutions before and after the filtration measured with a viscometer of the Ubbelohde type, we confirmed that the filtration neither changed the concentration of the test solution nor degraded the sample in it. The most concentrated solutions of the a-PMMA samples in acetonitrile were prepared in the following manner. The samples were optically purified by filtration of their solutions in acetone, as mentioned above, followed by drying at 50−60 °C for 3 days. Then the purified samples were dissolved in acetonitrile optically purified by filtration through a membrane of pore size 0.1 μm. The solutions so prepared were allowed to stand in the dark at ca. 50 °C for 3 days, being stirred by shaking the vessel gently twice a day. All the solutions of lower concentrations were obtained by sequential dilution. The weight concentrations of the test solutions were determined gravimetrically and converted to the mass concentrations by using the densities of the solutions.

The values of M_w and $\langle S^2\rangle^{1/2}$ thus determined are given in the second and fourth columns of Table 1, respectively, where the values for the a-PS sample F550-a in cyclohexane at 34.5 °C had been determined previously.[8] For each sample, the figures with and without parentheses represent the values in its good and Θ solvents, respectively, and are seen to agree with each other within experimental error. We note that the ratio of M_w to the number-average molecular weight M_n could be determined from analytical gel permeation chromatography (GPC) only for the a-PMMA sample Mr48, its value being given in the third column of Table 1. Although the values of M_w/M_n for the other samples could not be determined with sufficient accuracy because of the lack of the GPC calibration curve in the necessary range, their molecular weight distributions may be considered as narrow ($M_w/M_n < 1.1$) as that of Mr48.

Dynamic Light Scattering. DLS measurements were carried out to determine the translational diffusion coefficient D for the a-PS sample F850-a in cyclohexane at 34.5 °C (Θ) and for the two a-PMMA samples in acetonitrile at 44.0 °C (Θ). Measurements were also carried out to determine $\Omega(k)$ for the two a-PS samples in cyclohexane at 34.5 °C and for the two a-PMMA samples in acetonitrile at 44.0 °C.

The apparatus system, experimental procedure, and method of data analysis for D are the same as those described in the previous papers[10,11] except the data acquisition procedure for the measurements of the normalized autocorrelation function $g^{(2)}(t)$ of the scattered light intensity $I(t)$ at time t for a-PMMA, which is described below. For solutions of a-PMMA, some effects of residual aggregates of solute molecules on $g^{(2)}(t)$ had been observed in the previous study,[12] so that it was measured again by the use of the data acquisition procedure introduced therein[12] in order to remove the effects. In principle, the procedure consists of measuring successively a large number of sets of 264 accumulated values of $g^{(2)}(j\tau)$ with τ the sampling time ($j = 1, 2, ..., 264$), the accumulation for each set being made during 20 s. Only those sets of values which are free of such effects are then accumulated. The method of data analysis for obtaining $\Omega(k)$ is given in the next section.

For the determination of D for each sample, $g^{(2)}(t)$ was measured at five concentrations and at five or six scattering angles θ ranging from 15 to 30°. For the determination of $\Omega(k)$, on the other hand, it was measured at $\theta = 20$, 25, 30, 60, 90, 120, and 150° for F550-a, F850-a, and Mr48 and at $\theta = 30$, 45, 60, 90, 120, and 150° for Mr127. These measurements for each sample were carried out at five concentrations as in the case of the determination of D, but they were higher than those for D in order to increase photon counts at large θ. The sampling times adopted for the determination of D were 90−180 μs for F850-a, 9−12 μs for Mr48, and 22−27 μs for Mr127. For the determination of $\Omega(k)$, two measurements with different sampling times were carried out for each solution at each angle in order to cover a wide range of time and to check its possible dependence on the choice of the sampling time. The sampling times so adopted were 0.5−55 μs for F550-a, 0.5−90 μs for F850-a, and 0.2−20 μs for Mr48 and Mr127.

The test solutions of each sample were prepared in the same manner as in the case of SLS measurements. The values of the refractive index at 488 nm and of η_0 used are 1.424 and 0.768 cP, respectively, for cyclohexane at 34.5 °C and 1.337 and 0.285 cP, respectively, for acetonitrile at 44.0 °C.

Results

Translational Diffusion Coefficient. The values of D determined in the present study are $4.6_6 \times 10^{-8}$ cm^2/s for the a-PS sample F850-a in cyclohexane at 34.5 °C (Θ) and $1.8_4 \times 10^{-7}$ and $1.1_2 \times 10^{-7}$ cm^2/s for the a-PMMA samples Mr48 and Mr127, respectively, in acetonitrile at 44.0 °C (Θ). The values of the hydrodynamic radius R_H calculated from the defining equation

$$R_H = k_B T/6\pi\eta_0 D \tag{1}$$

with the above values of D are given in the fifth column of Table 1 along with that previously determined for F550-a in cyclohexane at 34.5 °C.[8]

The values of the ratio ρ of $\langle S^2\rangle^{1/2}$ to R_H calculated from the values given in the fourth and fifth columns of Table 1 are 1.31 and 1.30 for F550-a and F850-a, respectively, and 1.29 and 1.30 for Mr48 and Mr127, respectively. Although the present values for a-PS are somewhat larger than the values 1.27−1.28 previously determined,[10] this difference may be regarded as arising from the fact that the a-PS samples used in the present study are broader in molecular weight distribution than the previous ones, for which $M_w/M_n = 1.01-1.03$. The present values of ρ for a-PMMA agree well with the previous ones, 1.30−1.31 within experimental error. Thus it may be concluded that both the SLS and DLS measurements also for the present samples having rather large M_w could be carried out successfully.

First Cumulant. Figure 1 shows plots of $(\eta_0/2k_BTk^3)$ $\ln[g^{(2)}(t) - 1]$ against t for the a-PS sample F850-a in cyclohexane at 34.5 °C (Θ) at the mass concentration $c = 3.64 \times 10^{-4}$ g/cm^3 and for the a-PMMA sample Mr127 in acetonitrile at 44.0 °C (Θ) at $c = 3.44 \times 10^{-4}$ g/cm^3, both at the scattering angle $\theta = 150°$. We note that k is given by

$$k = (4\pi/\tilde{\lambda}) \sin(\theta/2) \tag{2}$$

with $\tilde{\lambda}$ the wavelength of the incident light in the

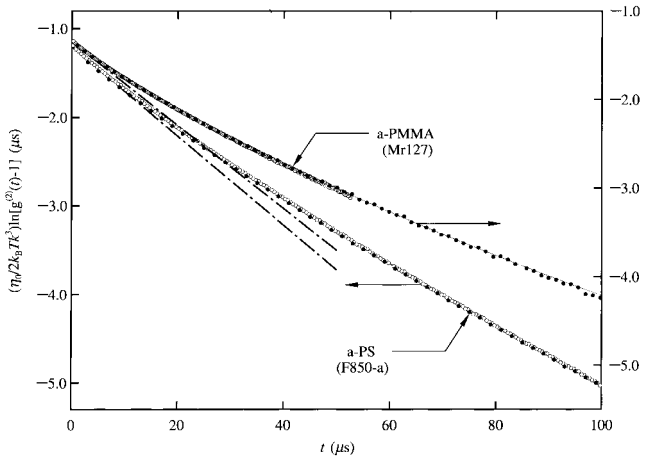

Figure 1. Plots of $(\eta_0/2k_BTk^3)\ln[g^{(2)}(t) - 1]$ against t for a-PS (F850-a) in cyclohexane at 34.5 °C (Θ) at $c = 3.64 \times 10^{-4}$ g/cm^3 and for a-PMMA (Mr127) in acetonitrile at 44.0 °C (Θ) at $c = 3.44 \times 10^{-4}$ g/cm^3, both at $\theta = 150°$. The filled and unfilled circles represent the values obtained with the sampling time $\tau = 2.0$ and 0.5 μs, respectively, for a-PS and with = 0.7 and 0.2 μs, respectively, for a-PMMA. The solid curves represent the best-fit empirical values determined by CONTIN, and the dot−dashed straight lines indicate the respective initial tangents (see the text).

solvent. The filled and unfilled circles represent the values obtained with the sampling time $\tau = 2.0$ and 0.5 μs, respectively, for F850-a and with $\tau = 0.7$ and 0.2 μs, respectively, for Mr127. We note that for Mr127 with $\tau = 0.7$ μs we have plotted only the values with $t = (2n - 1)\tau$ ($n = 1, 2, ...$), for convenience. Since the decay rate of the (observed) (1/2) $\ln[g^{(2)}(t) - 1]$ for Mr127 is about three times as large as that for F850-a due to the difference between the η_0 values of the respective Θ solvents, the values of τ adopted for a-PMMA are smaller than those for a-PS. In the measurements for each solution at each angle, we chose one of τ's to be so long that (1/2) $\ln[g^{(2)}(t) - 1]$ completely decayed to zero in the observed range of time, i.e., 0 to 264 (the channel number of the correlator used) × τ s, and the other to be about one-third of the former.

It is seen from Figure 1 that for Mr127 the two sets of plotted values with $\tau = 0.7$ and 0.2 μs agree well with each other, while for F850-a the values with $\tau = 2.0$ μs are somewhat smaller than those with $\tau = 0.5$ μs and the former initial decay rate seems slightly smaller than the latter. The reason for this difference is not clear. In this connection, it may be pertinent to make the following remark. From an analysis on the basis of a multimode version of Jakeman's analysis[13] of the size effect of τ on the observed (1/2) $\ln[g^{(2)}(t) - 1]$, the details of which are omitted, it can be shown that an increase in τ enhances the contribution of fast decay modes, so that the observed initial decay rate of (1/2) $\ln[g^{(2)}(t) - 1]$ may be considered to increase with increasing τ if there is no other source. However, this cannot explain the above observation.

The first cumulant $\Omega(k)$ defined as the initial decay rate of the dynamic structure factor $S(k, t)$, i.e., $\Omega(k) \equiv -[d(\ln S(k, t))/dt]_{t=0}$ may be written in terms of $g^{(2)}(t)$ as follows:

$$\Omega(k) = -\left[\frac{d}{dt}\left\{\frac{1}{2}\ln[g^{(2)}(t) - 1]\right\}\right]_{t=0} \quad (3)$$

Then the value of the initial tangent at $t = 0$ of each plot in Figure 1 corresponds to the value of $-\eta_0\Omega(k)/k_BTk^3$. It is seen that $\eta_0\Omega(k)/k_BTk^3$ is definitely larger for a-PS (irrespective of the value of τ) than for a-PMMA.

Table 2. Values of $\Omega(k)$ and $\eta_0\Omega(k)/k_BTk^3$ for Polystyrene in Cyclohexane at 34.5 °C (Θ) and Poly(methyl methacrylate) in Acetonitrile at 44.0 °C (Θ)

sample	θ, deg	10^3k, Å^{-1}	$\Omega(k)$, s^{-1}	$\eta_0\Omega(k)/k_BTk^3$
F550-a	20	0.637	$2.2_5 \times 10^2$	0.157
	25	0.794	$3.5_7 \times 10^2$	0.129
	30	0.949	$5.1_4 \times 10^2$	0.109
	60	1.833	$2.2_8 \times 10^3$	0.066_9
	90	2.593	$5.4_2 \times 10^3$	0.056_2
	120	3.176	$9.2_9 \times 10^3$	0.052_5
	150	3.542	$1.2_7 \times 10^4$	0.051_6
F850-a	20	0.637	$1.9_5 \times 10^2$	0.136
	25	0.794	$3.1_5 \times 10^2$	0.114
	30	0.949	$4.6_4 \times 10^2$	0.098_1
	60	1.833	$2.1_0 \times 10^3$	0.061_7
	90	2.593	$5.1_9 \times 10^3$	0.053_8
	120	3.176	$9.1_5 \times 10^3$	0.051_7
	150	3.542	$1.2_5 \times 10^4$	0.051_0
Mr48	20	0.598	$6.7_6 \times 10^2$	0.206
	25	0.745	$1.0_7 \times 10^3$	0.168
	30	0.891	$1.5_2 \times 10^3$	0.140
	60	1.721	$6.3_8 \times 10^3$	0.081_4
	90	2.434	$1.4_3 \times 10^4$	0.064_5
	120	2.982	$2.3_4 \times 10^4$	0.057_5
	150	3.326	$3.0_0 \times 10^4$	0.053_1
Mr127	30	0.891	$9.9_4 \times 10^2$	0.091_4
	45	1.318	$2.4_3 \times 10^3$	0.069_2
	60	1.721	$4.5_9 \times 10^3$	0.058_6
	90	2.434	$1.1_3 \times 10^4$	0.051_1
	120	2.982	$1.9_4 \times 10^4$	0.047_7
	150	3.326	$2.6_5 \times 10^4$	0.046_9

The determination of $\Omega(k)$ from the observed values of (1/2) $\ln[g^{(2)}(t) - 1]$, i.e., by extrapolating the latter to $t = 0$ with a proper set of basis functions has been made by the use of the Fortran program package CONTIN[14] supplied by Brookhaven Instruments. It consists of expressing $[g^{(2)}(t) - 1]^{1/2}$ by a superposition of exponential decay functions $e^{-\gamma_i t}$ ($i = 1, 2, ..., n_f$) with a given set of decay rates $\{\gamma_i\}$, the amplitude A_i of $e^{-\gamma_i t}$ being determined by the method of least squares under the condition $A_i \geq 0$ (for all i) and with the principle of "parsimony," i.e., smoothness with a minimum number of peaks of A_i as a function of γ_i (or log γ_i).[14] In practice, we have put $\gamma_i = 10^{\alpha+(i-1)(\beta-\alpha)/(n_f-1)}$ s^{-1} with $n_f = 25$ and with properly chosen values of the parameters α and β. In the extrapolation, we have neglected the data points for $t \lesssim 5$ μs, considering the fact that the effect of after pulses may remain up to a few microseconds.

In Figure 1, the solid curves represent the values of the best-fit functions so determined for F850-a with $\tau = 0.7$ μs and for Mr127, the curve for the former being hidden by the data points, where we have chosen $\alpha = 3$ and $\beta = 6$ for F850-a and $\alpha = 3.3$ and $\beta = 6.3$ for Mr127. The dot−dashed straight lines represent the respective initial tangents. The values of $\Omega(k)$ ($\eta_0\Omega(k)/k_BTk^3$) evaluated from these tangents are $1.23_1 \times 10^4$ s^{-1} (0.0501) and 2.46×10^4 s^{-1} (0.0435) for a-PS and a-PMMA, respectively. For comparison, we have evaluated $\Omega(k)$ for F850-a with $\tau = 2.0$ μs, and the result is $1.23_4 \times 10^4$ s^{-1} ($\eta_0\Omega(k)/k_BTk^3$= 0.502) and agrees with that with $\tau = 0.7$ μs.

For each sample at each scattering angle θ, $\Omega(k)$ at infinite dilution has been determined by extrapolating linearly the data so evaluated at finite concentrations c to $c = 0$. In Table 2 are given the values of $\Omega(k)$ and $\eta_0\Omega(k)/k_BTk^3$ so determined. It is interesting to note that the slope of the straight line of extrapolation

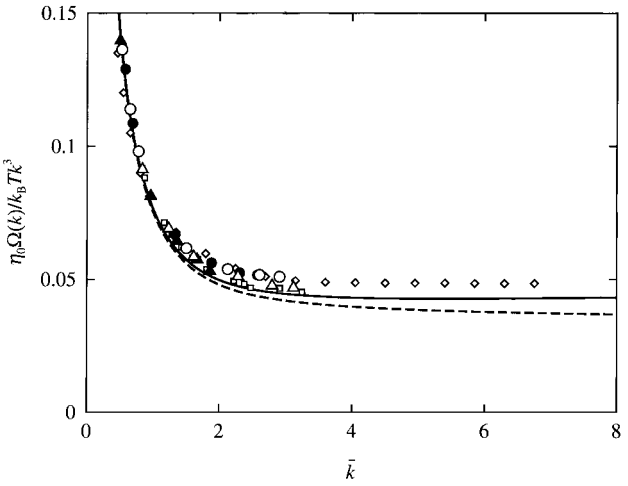

Figure 2. Plots of $\eta_0\Omega(k)/k_BTk^3$ against the reduced magnitude $\bar{k}$ of the scattering vector. The filled and unfilled circles represent the present experimental values for the a-PS samples F550-a and F850-a, respectively, in cyclohexane at 34.5 °C (Θ), and the filled and unfilled triangles, for the a-PMMA samples Mr48 and Mr127, respectively, in acetonitrile at 44.0 °C (Θ). For comparison, there are also shown the results obtained by Han and Akcasu[15] for a-PS in cyclohexane at 35.0 °C (Θ) (diamonds) and by Tsunashima et al.[16] for a-PS in *trans*-decalin at 20.4 °C (Θ) (square), respectively. The solid and dashed curves represent the HW theoretical values for a-PS and a-PMMA, respectively.

decreases with increasing θ and that $\Omega(k)$ becomes almost independent of c at $\theta = 150°$. This result may be considered rather natural, considering the fact that $\Omega(k)$ at large k reflects internal motions and therefore is not sensitive to change of c.

Discussion

Nonuniversality. Figure 2 shows plots of $\eta_0\Omega(k)/k_BTk^3$ against the reduced magnitude $\bar{k}$ of the scattering vector defined by

$$\bar{k} \equiv \langle S^2\rangle^{1/2}k \tag{4}$$

The filled and unfilled circles represent the present experimental values for the a-PS samples F550-a and F850-a, respectively, in cyclohexane at 34.5 °C (Θ) and the filled and unfilled triangles for the a-PMMA samples Mr48 and Mr127, respectively, in acetonitrile at 44.0 °C (Θ). For comparison, there are also shown the results obtained by Han and Akcasu[15] for a-PS in cyclohexane at 35.0 °C (diamonds) and by Tsunashima et al.[16] for a-PS in *trans*-decalin at 20.4 °C (squares).

It is seen that the present values for a-PMMA are appreciably (ca. 10%) smaller than those for a-PS in the k^3 -region ($\bar{k} \gtrsim 2$) where $\Omega(k)$ is proportional to k^3. As also seen from Figure 1, this difference is not within the limits of experimental error, thus leading to the conclusion that the universality in the k^3 -region cannot be realized even for such large M_w ($\simeq 10^7$). Note that the universality would be, of course, realized in the (Gaussian) limit of $M_w \to \infty$, as required theoretically. The present results for a-PS are close to those obtained by Han and Akcasu but somewhat larger than those by Tsunashima et al. This difference may possibly be due to the difference in the data treatment between the laboratories.

Comparison with the HW Theory. For the (discrete) dynamic HW chain model,[4] which is composed of N identical rigid subbodies joined successively with bonds of fixed length a, each subbody having translational and rotatory friction coefficients ζ_t and ζ_r, the quantity $\eta_0\Omega(k)/k_BTk^3$ may be written in the form[5]

$$\eta_0\Omega(k)/k_BTk^3 = (1/6\pi)[\rho/\bar{k} + F(\bar{k})/\bar{k}] \tag{5}$$

where

$$F(\bar{k}) = \frac{2\langle S^2\rangle^{1/2}}{3r_1r_2aS(\bar{k}, 0)}\sum_{K=1}^{N} A_K(\bar{k})(|R^{00}{}_{1,K}|^2\tilde{\lambda}^0{}_{1,K} + |R^{(-1)0}{}_{1,K}|^2\tilde{\lambda}^{(-1)}{}_{1,K}) \tag{6}$$

with

$$S(\bar{k}, 0) = \frac{1}{N+1} + \frac{2}{(N+1)^2}\sum_{n=1}^{N}(N-n+1)\times \exp\left[-\frac{\bar{k}^2}{6}\frac{\langle R^2(n\Delta s)\rangle}{\langle S^2(L)\rangle}\right] \tag{7}$$

$$A_K(\bar{k}) = \frac{1}{4(N+1)^2}\mathrm{cosec}^2\left[\frac{K\pi}{2(N+1)}\right]\times \left\{1 + \frac{2}{N+1}\sum_{n=1}^{N}\left[(N-n+1)\cos\left(\frac{nK\pi}{N+1}\right) - \mathrm{cosec}\left(\frac{K\pi}{N+1}\right)\sin\left(\frac{nK\pi}{N+1}\right)\right]\exp\left[-\frac{\bar{k}^2}{6}\frac{\langle R^2(n\Delta s)\rangle}{\langle S^2(L)\rangle}\right]\right\} \tag{8}$$

In eq 6, $\tilde{\lambda}^j{}_{1,K}$ are the dimensionless (reduced) eigenvalues defined by $\tilde{\lambda}^j{}_{1,K} = \zeta_r\,\lambda^j{}_{1,K}/k_BT$, where the (unreduced) eigenvalues $\lambda^j{}_{1,K}$ of the diffusion operator associated with the coarse-grained dynamic HW chain[4,17] are given by eq 47 of ref 18, and $R^{j0}{}_{1,K}$ are given by eq 23 of ref 5. The quantities $\tilde{\lambda}^j{}_{1,K}$ and $R^{j0}{}_{1,K}$ may be numerically evaluated for a given set of model parameters. There are four parameters other than N, ζ_t, and ζ_r to describe the model, i.e., the constant differential-geometrical curvature κ_0 and torsion τ_0 of the characteristic helix of the corresponding continuous HW chain of total contour length L, the static stiffness parameter λ^{-1}, and $\Delta s = L/N$. (Recall that a is uniquely related to Δs, which is chosen to be equal to the contour length per repeat unit of a given polymer chain in the case of flexible polymers.) We note that the values of the dimensionless parameters $r_1 = \zeta_t/3\pi\eta_0 a$ and $r_2 = \zeta_r/a^2\zeta_t$ instead of those of ζ_t and ζ_r themselves are required to calculate $\tilde{\lambda}^j{}_{1,K}$. In eqs 7 and 8, $\langle R^2(L)\rangle$ and $\langle S^2(L)\rangle$ are the mean-square end-to-end distance and mean-square radius of gyration, respectively, of the corresponding continuous HW chain of contour length L and are given by

$$\langle R^2(L)\rangle = \frac{4+\tau_0{}^2}{r^2}L - \frac{\tau_0{}^2}{2\nu^2} - \frac{2\kappa_0{}^2(4-\nu^2)}{\nu^2r^4} + e^{-2L}\left\{\frac{\tau_0{}^2}{2\nu^2} + \frac{2\kappa_0{}^2}{\nu^2r^4}[(4-\nu^2)\cos(\nu L) - 4\nu\sin(\nu L)]\right\} \tag{9}$$

$$\langle S^2(L)\rangle = \frac{{\tau_0}^2}{\nu^2}\left[\frac{L}{6} - \frac{1}{4} + \frac{1}{4L} - \frac{1}{8{L}^2}(1 - e^{-2L})\right] + \frac{{\kappa_0}^2}{\nu^2}\left[\frac{L}{3r}\cos\phi - \frac{1}{r^2}\cos(2\phi) + \frac{2}{r^3 L}\cos(3\phi) - \frac{2}{r^4{L}^2}\cos(4\phi) + \frac{2}{r^4{L}^2}e^{-2L}\cos(\nu L + 4\phi)\right] \quad (10)$$

with

$$\nu = ({\kappa_0}^2 + {\tau_0}^2)^{1/2} \quad (11)$$

$$r = (4 + \nu^2)^{1/2} \quad (12)$$

$$\phi = \cos^{-1}(2/r) \quad (13)$$

where all lengths are measured in units of λ^{-1}, for simplicity.

In Figure 2, the solid and dashed curves represent the HW theoretical values calculated from eq 5 for a-PS and a-PMMA, respectively. In the calculation we have used $\lambda^{-1}\kappa_0 = 3.0$, $\lambda^{-1}\tau_0 = 6.0$, and $\lambda^{-1} = 20.6$ Å for a-PS[4,19] and $\lambda^{-1}\kappa_0 = 4.0$, $\lambda^{-1}\tau_0 = 1.1$, and $\lambda^{-1} = 57.9$ Å for a-PMMA,[4,20] which have been determined experimentally from an analysis of the M_w dependence of the (unperturbed) $\langle S^2\rangle$. The subbody corresponds to a repeat unit of a given polymer chain, as mentioned above, and then the values of $\lambda\Delta s$ have been taken to be 0.14 and 0.048 for a-PS and a-PMMA, respectively, which have been calculated from $\Delta s = M_0/M_L$ with the values 104 and 100 of the molecular weight M_0 of the repeat unit for a-PS and a-PMMA, respectively, and with the values 35.8 and 36.3 Å^{-1} of the shift factor M_L (as defined as the molecular weight per unit contour length) for a-PS[19] and a-PMMA,[20] respectively. Further, we have chosen r_1 and r_2 to be 1 and 10, respectively, which may be of reasonable order, and $N + 1$ to be 10^4, which corresponds to the limit of the capacity of the computer used. The calculation also requires the value of ρ, for which in the present theoretical framework we should use the Kirkwood value $8/3\pi^{1/2} = 1.505$ (refs 21 and 22) for the center of mass of the infinitely long Gaussian chain (in the nondraining limit). As is well known, however, the experimental values of ρ for flexible polymers with very large M_w are appreciably smaller than the Kirkwood value; the present experimental values of ρ are 1.30_5 and 1.29_5 for a-PS and a-PMMA, respectively, each of which is the average of the values obtained for the two samples. Thus we have used these experimental values for the theoretical calculation, as done before.[5] (For the general behavior of the theoretical values of the reduced Ω such as the N dependence, see ref 5.)

Although the theoretical values are smaller than the experimental ones in the k^3 -region for both a-PS and a-PMMA, the theory may explain well the experimental result that $\eta_0\Omega(k)/k_BTk^3$ is larger for a-PS than for a-PMMA in this region, indicating that the HW theory takes proper account of the effect of chain stiffness and local chain conformation also for the present problem.

Finally, it is pertinent to refer to the theoretical study of the effect of chain stiffness on $\Omega(k)$ made by Benmouna et al.[23] on the basis of the "sliding-rod" model, i.e., a hybrid of the rod and the Gaussian chain. (It is an incomplete version of the Kratky−Porod wormlike chain.[24]) Although their model also predicts the breakdown of the universality, it cannot give a consistent explanation of the behavior of the scattering function and hydrodynamic radius, especially for a-PMMA, since it cannot take account of the effect of local chain conformation.

Conclusion

The first cumulant $\Omega(k)$ as a function of the magnitude k of the scattering vector has been determined for a-PS in cyclohexane at 34.5 °C (Θ) and a-PMMA in acetonitrile at 44.0 °C (Θ), these polymer chains being remarkably different from each other in chain stiffness and local chain conformation. In consistence with the theoretical prediction on the basis of the HW chain model,[5] the universality of the plots of the reduced first cumulant $\eta_0\Omega(k)/k_BTk^3$ against the reduced magnitude $\langle S^2\rangle^{1/2}k$ of the scattering vector cannot be realized even for the samples having very high molecular weights ($\simeq 10^7$). The indication is that the effect of chain stiffness and local chain conformation on the internal motions is still appreciable even for such large molecular weights where the global behavior may be completely described by the Gaussian chain.

References and Notes

(1) de Gennes, P. G. *Physics* **1967**, *3*, 37.
(2) Dubois-Violette, E.; de Gennes, P. G. *Physics* **1967**, *3*, 181.
(3) Akcasu, Z.; Gurol, H. *J. Polym. Sci., Polym. Phys. Ed.* **1976**, *14*, 1.
(4) Yamakawa, H. *Helical Wormlike Chains in Polymer Solutions*; Springer: Berlin, 1997.
(5) Yoshizaki, T.; Osa, M.; Yamakawa, H. *J. Chem. Phys.* **1997**, *106*, 2828.
(6) Stockmayer, W. H.; Hammouda, B. *Pure Appl. Chem.* **1984**, *56*, 1372.
(7) Schmidt, M.; Stockmayer, W. H. *Macromolecules* **1984**, *17*, 509.
(8) Arai, T.; Abe, F.; Yoshizaki, T.; Einaga, Y.; Yamakawa, H. **1995**, *28*, 5458.
(9) Berry, G. C. *J. Chem. Phys.* **1966**, *44*, 4550.
(10) Konishi, T.; Yoshizaki, T.; Yamakawa, H. *Macromolecules* **1991**, *24*, 5614.
(11) Osa, M.; Abe, F.; Yoshizaki, T.; Einaga, Y.; Yamakawa, H. *Macromolecules* **1996**, *29*, 2302.
(12) Dehara, K.; Yoshizaki, T.; Yamakawa, H. *Macromolecules* **1993**, *26*, 5137.
(13) Jakeman, E. In *Photon Correlation and Laser Beating Spectroscopy*; Cummins, H. Z., Pike, E. R., Eds.; Plenum Press: New York, 1974.
(14) Provencher, S. W. *Comput. Phys. Commun.* **1982**, *27*, 213.
(15) Han, C. C.; Akcasu, A. Z. *Macromolecules* **1981**, *14*, 1080.
(16) Tsunashima, Y.; Nemoto, N.; Kurata, M. *Macromolecules* **1983**, *16*, 1184.
(17) Yoshizaki, T.; Yamakawa, H. *J. Chem. Phys.* **1996**, *104*, 1120.
(18) Yoshizaki, T.; Osa, M.; Yamakawa, H. *Macromolecules* **1996**, *105*, 11268.
(19) Abe, F.; Einaga, Y.; Yoshizaki, T.; Yamakawa, H. *Macromolecules* **1993**, *26*, 1884.
(20) Tamai, Y.; Konishi, T.; Einaga, Y.; Fujii, M.; Yamakawa, H. *Macromolecules* **1990**, *23*, 4067.
(21) Kirkwood, J. G.; Riseman, J. *J. Chem. Phys.* **1948**, *16*, 565.
(22) Kirkwood, J. G. *Recl. Trav. Chim. Pays-Bas* **1949**, *68*, 649; *J. Polym. Sci.* **1954**, *12*, 1.
(23) Benmouna, M.; Akcasu, A. Z.; Daoud, M. *Macromolecules* **1980**, *13*, 1703.
(24) Kratky, O; Porod, G. *Recl. Trav. Chim. Pays-Bas* **1949**, *68*, 1106.

MA980354Z